energies

MDPI

*Article*

# 2-Stroke RCCI Engines for Passenger Cars

**Enrico Mattarelli [1,*], Carlo Alberto Rinaldini [1], Luca Marmorini [2], Stefano Caprioli [1], Francesco Legrottaglie [1] and Francesco Scrignoli [1]**

[1] Dipartimento di Ingegneria "Enzo Ferrari", Università degli Studi di Modena e Reggio Emilia, via Pietro Vivarelli 10, 41125 Modena, Italy; carloalberto.rinaldini@unimore.it (C.A.R.); stefano.caprioli@unimore.it (S.C.); francesco.legrottaglie@unimore.it (F.L.); francesco.scrignoli@unimore.it (F.S.)
[2] Marmotors s.r.l., 52100 Arezzo, Italy; marmorix@mac.com
* Correspondence: enrico.mattarelli@unimore.it; Tel.: +39-05-9205-6151

**Abstract:** Reactivity Controlled Compression Ignition (RCCI) is one of the most promising solutions among the low temperature combustion concepts, in terms of thermal efficiency and pollutant emissions. However, for values of brake mean effective pressure higher than 10 bar, in-cylinder peak pressure rise rates tend to be too high, limiting the specific power of any 4-Stroke (4S) engine. Such a limitation can be canceled by moving to the 2-Stroke (2S) cycle. Among many alternatives, the "Uniflow" scavenging system with exhaust poppet valves on the cylinder head allows the designer to reproduce the same identical combustion patterns of a 4-stroke RCCI engine, while increasing the indicated power output. The goal of the paper is to explore the potential of a 2-stroke RCCI engine, on the basis of a comprehensive experimental campaign carried out on a modified automotive 2.0 L, 4-stroke, four-cylinder, four-valve diesel engine. The developed prototype can run with one cylinder operating in 4-stroke RCCI mode (gasoline–diesel), while the others work in the standard diesel mode. A One Dimensional-Computational Fluid Dynamics (1D-CFD) model has been built to predict the performance of the same prototype, when operating all four cylinders in RCCI mode. In parallel, an equivalent 2-stroke RCCI virtual engine has been developed, by means of 1D-CFD simulations and empirical assumptions. A numerical comparison between the 4S and the 2S engines is finally presented, in terms of performance and emissions at full load. The study demonstrates that a 2S RCCI engine can maintain all of the advantages of the RCCI combustion, strongly reducing the penalization in terms of performance, in comparison to a standard 4S diesel engine.

**Keywords:** automotive diesel engine; 4-stroke; RCCI (gasoline – diesel); experimental engine characterization; 1D-CFD; 2-stroke; Uniflow scavenging

**Citation:** Mattarelli, E.; Rinaldini, C.A.; Marmorini, L.; Caprioli, S.; Legrottaglie, F.; Scrignoli, F.. 2-Stroke RCCI Engines for Passenger Cars. *Energies* **2022**, *15*, 1173. https://doi.org/10.3390/en15031173

Academic Editors: Stephan P. Schmidt and Francesco Balduzzi

Received: 31 December 2021
Accepted: 1 February 2022
Published: 5 February 2022



## 1. Introduction

Anthropogenic Greenhouse Gas (GHG) emissions are considered the major cause of the current climate changes. So far, human activities are responsible of an average global warming of about 1.0 °C, compared to the pre-industrial era [1]. At the current rate of 0.2 °C per decade, global warming is likely to reach the critical threshold of 1.5 °C between 2030 and 2052 [2] and of 3 °C by 2100 [3]. For this reason, the 2021 edition of the United Nations Annual Climate Change Conference (COP26) urged member countries to halve their GNH emissions over the next decade and reach net zero carbon emissions by the middle of the century [4].

According to reference [1], in 2016 the road transport sector was responsible of about 12% of the global $CO_2$ equivalent emissions. Even if the solution of the problem cannot be found by focusing on this field only, a change of course is mandatory. To achieve a significant reduction of GHG emissions in the short term, many different paths can be followed:

- Internal Combustion Engine (ICE) efficiency improvement: higher compression ratios, reduced pumping and frictions losses, waste heat recovery, innovative combustion concepts;
- Use of ultra-low-carbon print fuels: bio-fuels, e-fuels;
- Use of green hydrogen, pure or blended with other fuels in ICEs;
- Use of green hydrogen in fuel cells;
- Hybrid Electric Vehicles (HEV);
- Battery Electric Vehicles (BEV).

It is quite hard to believe that a single solution alone will be able to reduce the GHG emissions in the short and medium term, since every technology has its own pros and cons. As an example, the benefits of BEVs are strongly limited or cancelled at all, when the largest part of electric energy comes from the combustion of fossil fuels, as it occurs in most of the countries in the world. In addition, many issues regarding battery manufacturing, performance, charging, and disposal have not yet been fully addressed.

Therefore, the most likely scenario in the energy sector is the concomitance of different technologies, where the ICE can still play an important role, both as a stand-alone mover and in hybrid electric powertrains [5].

Diesel engines can be a key, since they are characterized by higher Brake Thermal Efficiency (BTE) compared to Spark Ignition (SI) engines, thus providing lower carbon dioxide ($CO_2$) emissions. Furthermore, diesel engines show considerably lower carbon monoxide (CO) and Unburnt Hydrocarbons (UHC) emissions.

The main technical drawback that affects diesel engines is represented by nitrogen oxides ($NO_x$) and Particulate Matter (PM) emissions, which impose cumbersome and expensive after-treatment systems. Moreover, the future vehicle emissions regulations will set even more stringent limits on pollutants, making the installation of these engines on passenger cars less and less sustainable, from an economic point of view.

A way for reducing $NO_x$ and PM emissions of diesel engines without compromising on BTE is represented by the Low Temperature Combustion (LTC) concepts [6]. Among them, Dual Fuel (DF) Reactivity Controlled Compression Ignition (RCCI) combustion, using port-injected gasoline as the low reactivity fuel and direct-injected diesel as the high reactivity one, has shown very promising results, i.e., ultra-low $NO_x$ and soot emissions, and outstanding BTE [7–12]. Moreover, RCCI is able to operate over a wider range of engine speeds and loads, compared to other LTC concepts, by controlling the local reactivity of the charge within the cylinder [13–16]. However, as engine load increases, peak in-cylinder pressure and Peak Pressure Rise Rate (PPRR) tend to become too high, limiting the RCCI operating range [17]. In order to expand the RCCI combustion mode up to high/full loads, different strategies have been explored.

Ma et al. [18] suggested that a double diesel injection strategy, with a delayed second injection, is more favorable for reducing PPRR, and hence extending RCCI operation to higher loads, compared to more conventional diesel injection strategies (two shots or single shot around the top dead center). The authors were able to achieve IMEP = 13.91 bar in RCCI mode, keeping the original Compression Ratio (CR).

Conversely, Molina et al. [19] extended RCCI operations to high loads by reducing CR. Furthermore, an early intake valve closing Miller cycle was implemented by means of a hydraulic Variable Valve Actuation (VVA) system. The authors also modified the injection strategy as a function of load. Their results suggest that a double diesel injection strategy suits well RCCI combustion from low (BMEP = 6 bar) to medium loads (BMEP = 12 bar), while a single shot injection strategy is better for high loads (BMEP > 17 bar).

The need for reducing CR in order to achieve high loads was confirmed also by Kavuri et al. [20], who performed a numerical optimization at two operating conditions: Low load–high speed (gross IMEP = 2 bar, 1800 rpm) and high load–low speed (gross IMEP = 20 bar, 1300 rpm). The study was carried out by means of a detailed three-dimensional (3D) Computational Fluid Dynamics (CFD) model, in combination with a Genetic Algorithm (GA). The optimization considered 28 different designs, including some geometric parameters of the piston bowl and of the diesel injector nozzle, as well as the control of air and fuel rates. The optimum value of CR was found at 13.1:1, adopting a bowl geometry characterized by two distinct regions, each one optimized for operating over a specific range of loads.

Benajes et al. [21], besides reducing CR from 17.5:1 to 15.3:1, adopted a Dual-Mode Dual-Fuel (DMDF) strategy. At low loads, a highly-premixed RCCI combustion was successfully applied for decreasing emissions and improving fuel efficiency. At high loads, combustion switches to the diffusive dual-fuel mode, for complying with the mechanical constraints (limit of PPRR). The DMDF strategy was numerically optimized by 3D-CFD simulations, governed by a GA, as described in [22]. The results revealed that, at low load, simultaneous improvement of fuel consumption and emissions can be obtained by enhancing the homogeneity of the charge. At mid load, fuel consumption can be improved by generating two high-reactivity regions within the cylinder (one above the piston lip and the second in the piston bowl). This permits to reduce the need for high intake temperature, with ensuing advantages on heat transfer losses. At high load, fuel consumption can be lowered by reducing the fraction on diesel fuel that burns in diffusive combustion mode.

A different method for keeping the benefits of the RCCI technology without penalization on engine brake power is to implement this combustion mode on a 2-Stroke (2S) engine. Thanks to the double cycle frequency, it is possible to enhance the performance without increasing neither the amount of injected fuel nor the peak of pressure rise rate. In theory, assuming the same speed, brake thermal efficiency and fuel rates, the power density can be doubled.

Obviously, it is necessary to select a proper design for the 2-stroke engine, in order to prevent some typical issues. Without the intake and the exhaust strokes, the fresh charge must be pumped into the cylinders by means of an external system, typically made up of a turbocharger coupled to a supercharger. The last one is necessary to start the engine, as well as to assist the turbocharger, especially at low engine speeds and low loads. The replacement of the exhaust gases with the fresh charge occurs when the piston is at bottom dead center (scavenging process); among many alternative solutions, the most widespread one on medium-large bore engines is the so-called "Uniflow" design [23]. It consists of a set of piston controlled ports located at the bottom of the cylinder liner, and a set of exhaust poppet valves installed on the engine head. Fuel can be injected directly into the cylinder, without any loss at the exhaust. This design, adopted on almost all of the large-bore low-speed 2-stroke engines (naval and steady plants) permits to reach excellent values of brake thermal efficiency (even higher than 50%), along with relatively high power density (in comparison to their 4-stroke counterparts) [23]. Even if the application of this design concept to small bore engines is not straightforward, many successful attempts have been made, in all of the automotive fields [24].

In the current study, only the "Uniflow" design was considered, for the reason that its combustion system can be identical to that of a conventional 4-stroke diesel engine, converted to operate in RCCI mode. The purpose of the paper is not to develop the best possible 2-stroke RCCI engine, but to evaluate the potential of the two-stroke cycle in general, when adopting this particular type of combustion mode. Since all the experimental measures were taken on a 4-stroke prototype, developed by the authors, the correspondence of the combustion system is a paramount condition for performing a straightforward comparison.

The authors are well aware of the challenges of designing and optimizing a uniflow engine, as reported in [25]. In comparison to a conventional 4-stroke diesel engine, particular care must be devoted to the design of the exhaust valves, operating at a double frequency (higher thermal and mechanical loads); specific solutions must be adopted to control the blow-by between piston and liner, as well as the wear of the piston rings, which are forced to slide on the inlet ports. Moreover, in comparison to large bore and low speed uniflow diesel engines, employed in steady plants and ships, small bore and high speed units are typically less efficient.

This article takes as a reference an automotive diesel engine by FCA (2.0 L, 4S, four-cylinder, four-valve, 125 kW@3500 rpm, Euro VI compliant). The experimental activity was divided into two phases. The first one consisted in a comprehensive characterization of the "donor" engine, using an open ECU programmed by the authors. In the second phase, the engine was modified, so that three cylinders could operate in standard diesel conditions, whereas the fourth was calibrated for RCCI operations. The experimental information was employed to calibrate a 1D-CFD engine model (using the GT-Power software [26]) of a full RCCI version (all cylinders operating in RCCI mode). Finally, by means of 1D-CFD simulations and empirical assumptions, an equivalent 2S RCCI engine was developed. A numerical comparison among the engines is presented in terms of brake performance at full load, while pollutant emissions are estimated on the basis of experimental data, collected on the 4-stroke RCCI prototype, integrated by some empirical hypotheses.

## 2. The Experimental Campaign

The experimental campaign was carried out at a steady dynamometer bench, equipped with an eddy current brake, on a prototype developed by the authors on the basis of a commercial diesel engine by FCA (named 2.0L JTD). The main engine characteristics are listed in Table 1. The supercharging system includes a Variable Geometry Turbine (VGT) and Charge Air Cooler (CAC), after the turbocharger compressor. The after-treatment equipment is made up of a Diesel Oxidation Catalyst (DOC), a Diesel Particulate Filter (DPF) and a Selective Catalytic Reduction device (SCR). Emission control is also supported by two exhaust gas recirculation systems: High-pressure (HP-EGR), linking the exhaust manifold before the turbine to the intake manifold, after CAC; low-pressure (LP EGR), connecting the exhaust pipe, after DPF to the turbocharger compressor inlet. The intake ports are equipped with a set of flaps, controlled by an actuator, for increasing the turbulence within the cylinders (Variable Swirl Actuator—VSA).

**Table 1.** Base engine specifications.

| Engine Type | Diesel, 4-Cylinder in-Line |
|---|---|
| Homologation | Euro 6 |
| Maximum Power | 125 kW @ 3500 rpm |
| Maximum Torque | 385 Nm @ 2000 rpm |
| Maximum Comb Pressure | 190 bar |
| Bore x Stroke | 83 × 90.4 mm |
| Connecting rod length | 145 mm |
| Squish Height | 0.72 mm |
| Pin Offset | 0.3 mm |
| Displacement | 1956 cc |
| Compression ratio | 16.5:1 |
| N° of valve per cylinder | 4 |
| Injection system | Common Rail |
| Inlet Valve Open | 341° CA ATDC |
| Inlet Valve Close | −139° CA ATDC |
| Exhaust Valve Open | 116° CA ATDC |
| Exhaust Valve Close | −340° CA ATDC |

The first step of the activity consisted in replacing the original Bosch ECU with an open one, enabling a flexible control of each cylinder, even in the presence of unconventional combustion systems. The new ECU was mapped in order to obtain the same performances of the original engine, when running on a conventional diesel combustion mode (referred to as CDC).

The experimental measures (pressure and temperature in the most important locations of the gas-dynamic circuit and of the cooling and lubricating systems, mass flow rates of air and fuel, brake torque, instantaneous in-cylinder pressure) taken in CDC mode at different speeds and loads permitted the accurate calibration of a 1D-CFD engine model (GT-Power).

The RCCI combustion system was only implemented on one of the four cylinders, while the remaining three were run in CDC mode. Figure 1b presents the new layout of the engine in "3 + 1" mode, while Figures 2 and 3 show the pictures of the modified intake manifold and of the RCCI exhaust piping, respectively.

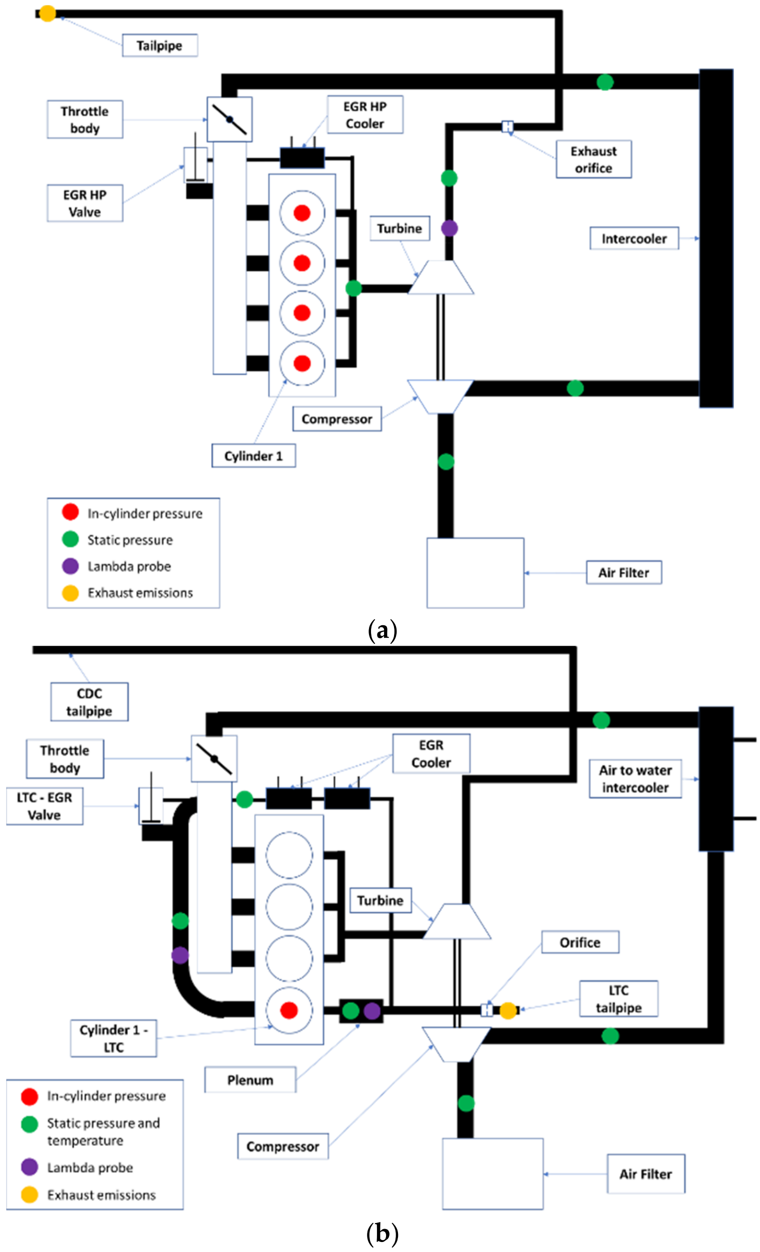


**Figure 1.** Layout of the engine running in CDC mode (**a**) and when running in the "3 + 1" mode (**b**).

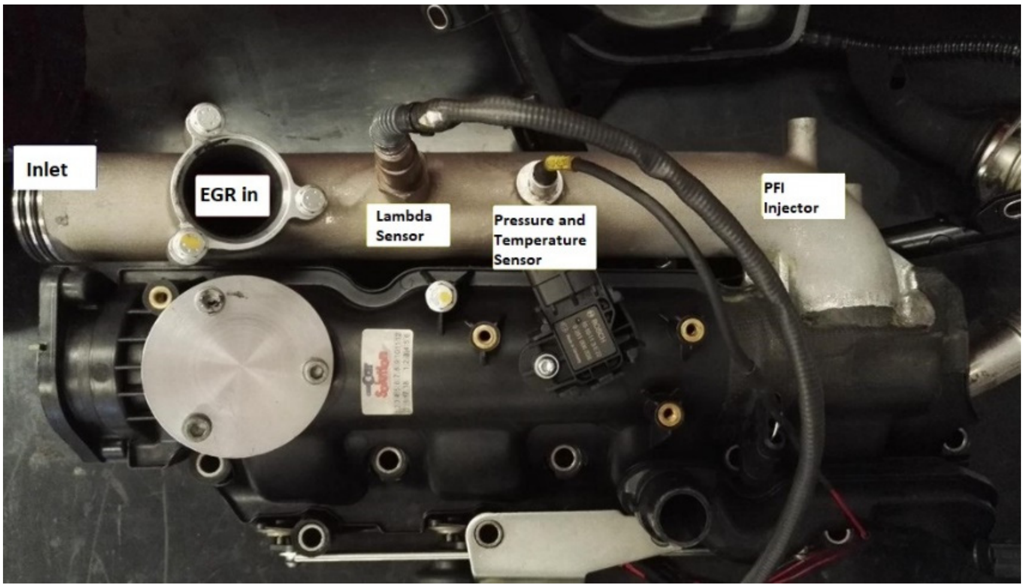


**Figure 2.** Picture of the modified intake manifold.

**Figure 3.** Picture of the exhaust piping relative to the RCCI cylinder, including the recirculation system and the exhaust gas cooler.

As visible in Figures 1–3, the three cylinders running in CDC mode are completely separated from the RCCI cylinder: after CAC, the air flow is split in two different paths; the VGT is powered only by the three CDC cylinders, while the fourth has its own piping. The exhaust gas is recirculated only in the RCCI cylinder, while the original LP-EGR system is not active. Figure 3 shows the flow split downstream of the RCCI cylinder: the front branch in the picture is the EGR pipe, including the liquid cooler and the EGR valve, whereas the rear pipe takes the gas to the ambient, throughout a plenum and a back-pressure valve. The last one is used to modify the EGR rate, in conjunction with the EGR valve.

As far as the intake system is concerned, a new pipe produced by addictive manufacturing is joined to the original manifold (see Figure 2). A Pico Racing fuel injector, type IWPR1, by Magneti Marelli (nominal flow rate at 10 bar: 690 cc/min) is installed at the end of the pipe, upstream of the RCCI cylinder. The EGR port is located as far as possible from the cylinder, in order to improve the mixing with air.

In comparison to a single cylinder prototype, the 3+1 engine configuration yields several advantages: First, it is not necessary to implement a specific air feed system, since the three cylinders running in CDC mode can always meet the boosting requirement of the RCCI cylinder; second, the engine keeps running even in case of misfire within the RCCI cylinder, a quite common situation during the calibration phase; last, but not least, a four-cylinder is not affected by the mechanical issues due to the torsional vibrations, typical of single-cylinders.

The composition of the charge in the RCCI cylinder is calculated by measuring the mass flow rate of gasoline and diesel, as well as the oxygen concentration within the intake and the exhaust manifolds of the RCCI cylinders (by means of two lambda sensors). Further information is provided by the analysis of the exhaust gas, carried out by means of a Horiba MEXA 1600 DEGR cabinet, which is able to measure CO, $CO_2$ (double measure), THC, NOx, and O2. The two measures of $CO_2$ in the inlet flow and in the exhaust flow permit an accurate estimation of the EGR rate. The measure of the exhaust gas composition is integrated by a smoke meter. The main characteristics of the most important instruments and sensors employed in the study are reviewed in Table 2.

**Table 2.** Main characteristics of the most relevant sensors and analyzers used in the experimental campaign.

| Parameter | Instrument | | Range | Unit | Accuracy | Reference |
|---|---|---|---|---|---|---|
| Cylinder Pressure | Kistler sensor 6113B | | 0–200 | bar | ±0.25% | full scale |
| Diesel mass flow rate | AVL mass flow meter | | 0–125 | kg/h | ±0.12% | full scale |
| Gasoline mass flow rate | Siemens Coriolis mass 6000 | | 0–250 | kg/h | ±0.10% | full scale |
| CO-$CO_2$ | Horiba MEXA 1600 DEGR—AIA 260 (NDIR) | CO-Low | 0–3000 | ppm | ±1% | full scale |
| | | CO-High | 0–10 | vol% | ±1% | full scale |
| | | $CO_2$ | 0–16 | vol% | ±1% | full scale |
| NOx and THC | Horiba MEXA 1600—FCA 266 (FID) | THC | 0–20,000 | ppm | ±1% | full scale |
| | | NOx | 0–5000 | ppm | ±1% | full scale |
| Lambda ($O_2$) | Lambda Sensor Bosch LSU 4.9 | | 0.65–10.11 | - | ±0.5% | @$\lambda$ = 1 |
| Smoke (FSN) | AVL smoke meter 415S | | 0–10 | FSN | ±3% | full scale @10 s sampling |

The tests on RCCI combustion covered all of the most important operating conditions, according to technical literature [12]: Low load (GIMEP up to 6 bar), medium load (GIMEP up to 9 bar), and high load (GIMEP up to 15 bar).

The three most important aspects for the control of RCCI combustion at a given load are:

1. The relative air-fuel ratio (lambda) of the premixed charge (air and gasoline);
2. The rate of EGR in the premixed charge;
3. The diesel injection strategy.

Besides SOI, it has been extensively investigated at the dynamometer bench the influence of: (1) Injection pressure; (2) number of shots and amount of fuel of each shot; (3) dwell time.

Differently from CDC, optimum values of SOI were found in the range between 40° and 80° CA before TDC. High injection pressures are needed to reduce the ignition retard.

EGR helps to smooth combustion roughness and reduce $NO_x$ emissions, but it has a slightly negative impact on PM, UHC, and CO.

As suggested by other authors [23], particular care was devoted to limit not only the peak cylinder pressure, $P_{max}$, but also the peak pressure rise rate, $(dP/d\theta)_{max}$. In commercial engines a maximum value of 10 bar/° can be tolerated. Considering racing applications,

$(dP/d\theta)_{max}$ may reach 20 bar/°. In this work, considering the use of state-of-the-art construction technologies, a maximum value of 13 bar/° is assumed as a reasonable limit.

The highest values of GIMEP were found with MFB50 to be just a few degrees after TDC, rather than at 8–10° ATDC, as in conventional combustion systems. This optimum condition corresponds also to the limit of peak pressure rise rate. This outcome is explained by the very fast heat release rate, just after the onset of combustion.

## 3. 1D-CFD Model of the RCCI 4-Cylinder Engine

The previously described experimental campaign is the base for the construction of a 1D-CFD 4-stroke (4S) four-cylinder engine model by GT-Power, where all cylinders run in RCCI mode.

As is well known, GT-Power [26] is a sort of virtual testing facility, able to predict all of the relevant engine performance parameters at any operating condition. A set of volumes is employed to represent the whole gas-dynamic system of the engine (zero/one dimensional space discretization), from the inlet ambient to the exhaust ambient, including the intake and exhaust ports and valves, the turbocharger with its own characteristic maps, etc.. The main input data are: Ambient conditions, engine speed, the opening of the throttle valve and of the EGR valve, the position of the swirl flaps, the diesel and gasoline mass flow rates, the experimental burn rates, and the mechanical losses associated with the moving components (crankshaft, pistons, connecting rods, etc.). GT-Power is an explicit code, so it calculates the change of the thermodynamic quantities throughout the gas-dynamic system at each time step. Convergence is reached when the cycle averaged quantities do not change from a cycle to the next one.

Before the analysis of the complete engine, the numerical model of the single cylinder running in RCCI mode was calibrated, considering the set of experimental data shown in Table 3. The selected points include five engine speeds (1500, 2000, 2500, 3000, 3500 rpm) and three loads (L = low, M = Medium, H = High). Each operating point is numbered from 1 to 15, for the sake of brevity.

**Table 3.** Operating conditions of the cylinder running in RCCI mode, selected for the calibration of the GT-Power engine model.

| **Case #** | **Load** | **Engine Speed [rpm]** | **EGR [%]** | **lambda [-]** | $\frac{m_{diesel}}{m_{tot}}$ **[-]** | **GIMEP [bar]** |
|---|---|---|---|---|---|---|
| 1 | L | 1500 | 0 | 2.25 | 10.16 | 6.19 |
| 2 | M | 1500 | 42 | 1.09 | 12.19 | 9.87 |
| 3 | H | 1500 | 45 | 1.02 | 12.19 | 10.77 |
| 4 | L | 2000 | 22 | 1.74 | 18.26 | 6.2 |
| 5 | M | 2000 | 35 | 1.21 | 8.13 | 8.65 |
| 6 | H | 2000 | 45 | 1.07 | 10.16 | 12.21 |
| 7 | L | 2500 | 17 | 1.96 | 16.24 | 7.26 |
| 8 | M | 2500 | 42 | 1.26 | 10.16 | 10.06 |
| 9 | H | 2500 | 38 | 1.06 | 8.13 | 13.96 |
| 10 | L | 3000 | 39 | 1.12 | 20.29 | 10.87 |
| 11 | M | 3000 | 36 | 1.06 | 20.29 | 12.73 |
| 12 | H | 3000 | 35 | 1.03 | 18.26 | 14.57 |
| 13 | L | 3500 | 32 | 1.46 | 10.16 | 10.00 |
| 14 | M | 3500 | 46 | 1.09 | 14.22 | 12.61 |
| 15 | H | 3500 | 38 | 1.06 | 18.26 | 13.33 |

For all of the selected cases, EGR and lambda are set in order to minimize pollutant emissions and maximize indicated thermal efficiency. At maximum load (H), the maximum fraction of diesel, divided by the total amount of fuel, is 18%. The maximum indicated work is measured at 3000 rpm (GIMEP = 14.6 bar).

The calibration basically consisted in tuning a few multipliers controlling fluid-dynamic losses and heat transfer. Further input data are the experimental burn rates and the pressures and temperatures across the cylinder. Figures 4 and 5 show the comparison between experimental data (GIMEP, volumetric efficiency, and EGR rate) and the correspondent numerical values. The reliability is very good for volumetric efficiency and GIMEP, as well as in terms of in-cylinder pressure traces (Figure 6). Some differences remain for the EGR rate, at a few points (7, 9, 15).

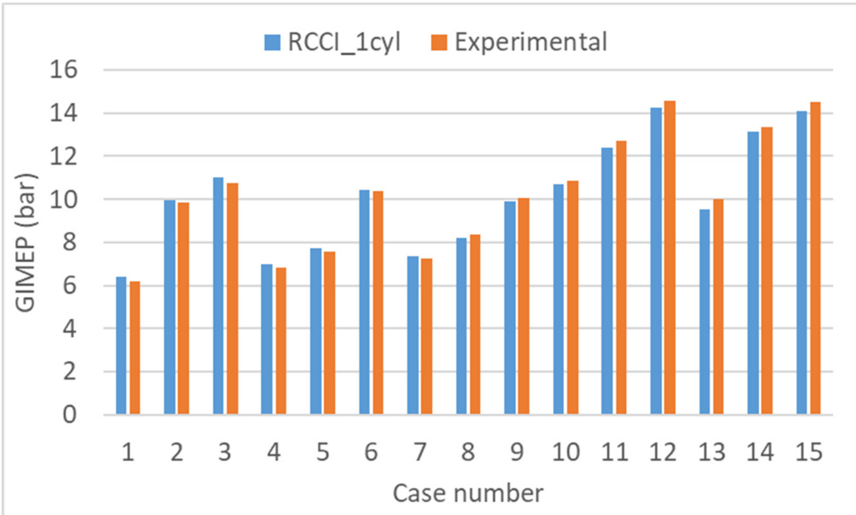


(**a**)

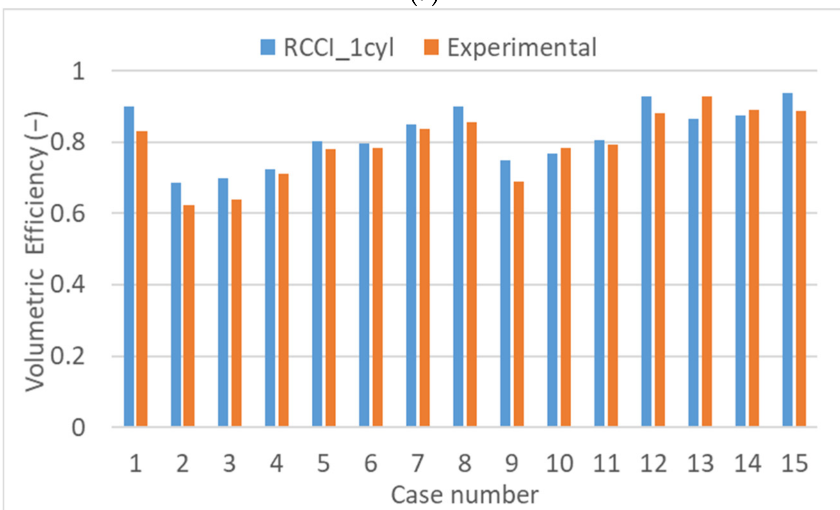


(**b**)

**Figure 4.** Gross IMEP (**a**) and volumetric efficiency (**b**): comparison between the calibrated 1D model and the experimental data.

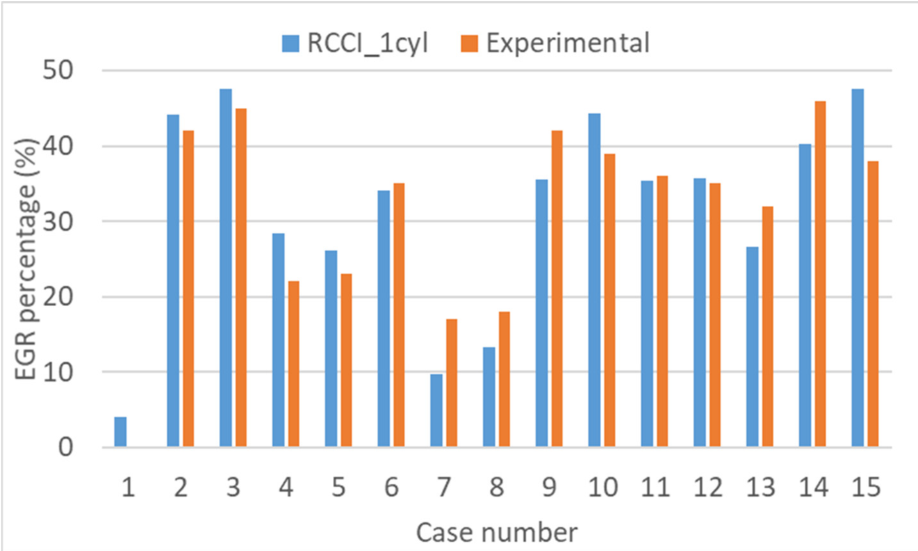


**Figure 5.** EGR rate comparison between the calibrated 1D model and experimental data.

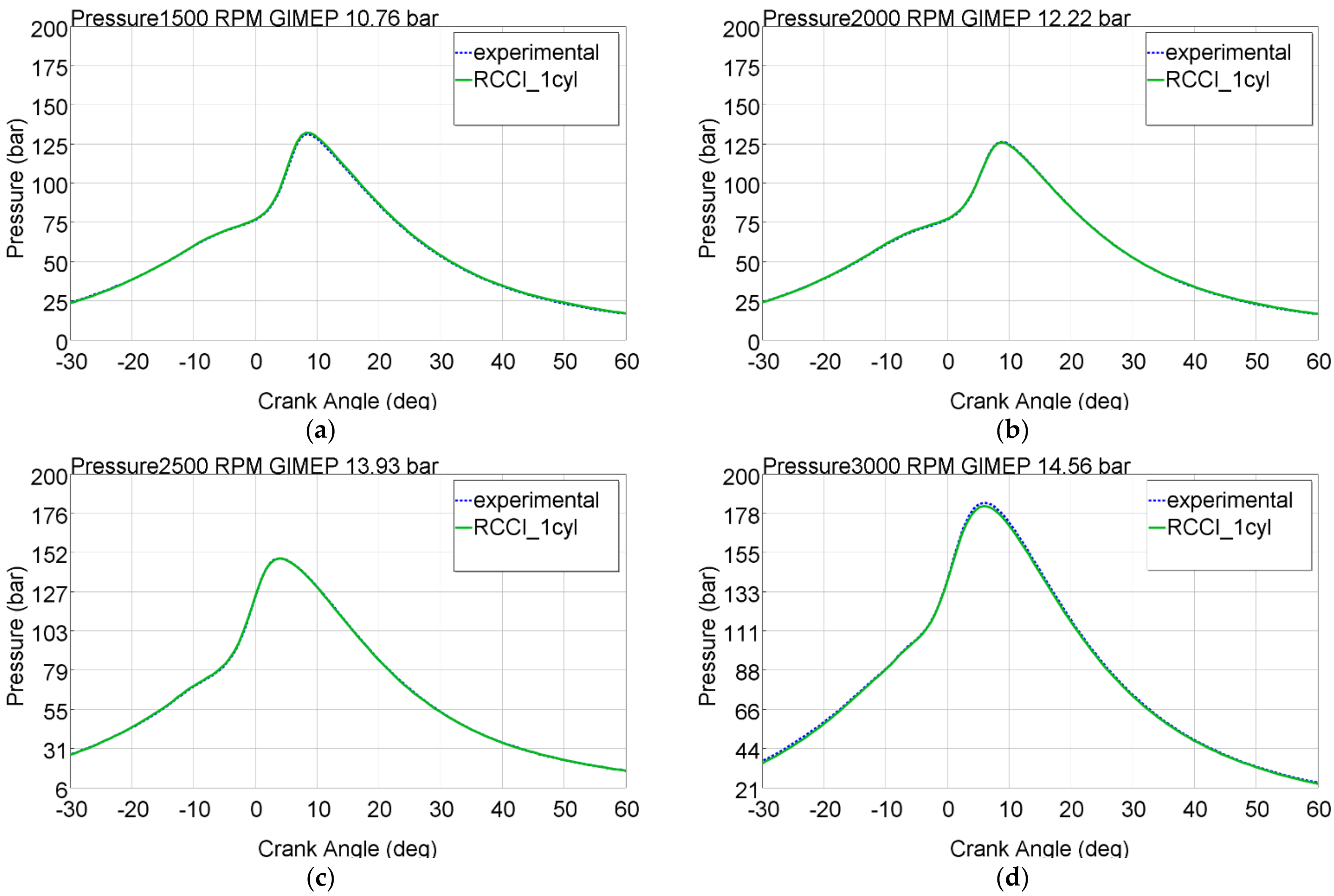

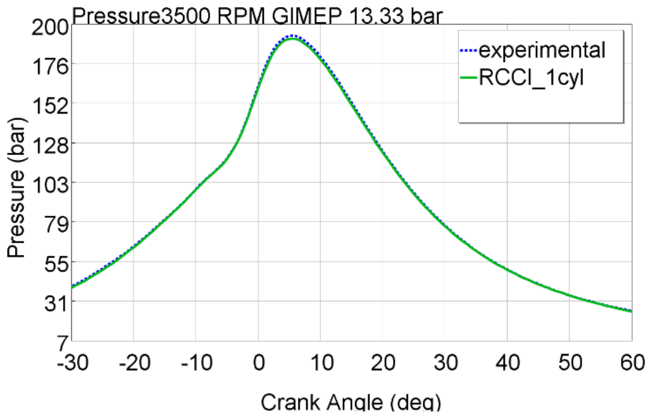

(**e**)

**Figure 6.** In-cylinder pressure comparison between experimental data and the simulated RCCI single cylinder at full load, speed: (**a**)1500 rpm; (**b**) 2000 rpm; (**c**) 2500 rpm; (**d**) 3000 rpm; (**e**) 3500 rpm.

The lack of agreement on EGR may also be due to a few accidental errors in the measurement chain, which are highly probable when the system is so complex. Despite this issue, the model is very reliable in the prediction of the performance outputs, as well as in the description of the effects of the combustion process (experimental and numerical pressure traces are perfectly superposed, at all the operating conditions analysed in the study). Moreover, all the numerical models employed in the study are derived from the same calibrated model, so that the the effects of this issue should be negligible in relative terms.

The calibrated CFD model of the RCCI cylinder was used to simulate a four-cylinder engine, at full load. The layout is the same as the original diesel engine; however a few modifications are needed. First, the new model includes a set of gasoline injectors. Second, a mechanical supercharger driven by the engine is added, in order to support the turbocharger at some critical operating conditions (low engine speed, high EGR rates). When not needed, the supercharger is bypassed and de-clutched. Third, the turbocharger is scaled, for a better matching to the new conditions.

The full load points for the four-cylinder, 4S engine correspond to cases 3, 6, 9, 12, and 15 (Table 3). The recirculated gas is provided by the standard LP-EGR system, while the value of the start of combustion is slightly adjusted in order to comply with the constraints on peak pressure rate rise and peak cylinder pressure. These parameters, as a matter of fact, determine the limit for the maximum performance outputs of the RCCI engine; a further increase of fuel rate would cause an engine failure.

## 4. The 2-Stroke Engine

The first purpose of the virtual 2S engine proposed in the study is to demonstrate the feasibility of an RCCI combustion system equivalent to the one experimentally developed on the 4-stroke prototype. Moreover, the numerical model permits to predict the engine performance outputs under the same identical hypotheses and design constraints adopted for the 4-stroke unit.

In order to maintain the same combustion patterns when passing from 4- to 2-stroke, at the same engine speed and fuel rate, the hypotheses listed below are made.

- The two engines share: Bore, stroke, number of cylinders, and geometry of the combustion chamber (shape of the bowl and cylinder head, squish clearance);
- The exhaust valve lift profile and timing of the 4S engine are modified, in order to operate according to the 2S cycle (double rotational speed, shorter opening duration, maximum lift around BDC);
- The intake valves and ports of the 4S engine are converted into exhaust valves, operating as described above;

- The set of inlet ports of the 2S engine is designed in order to provide the same swirl ratio within the cylinder, occurring at the intake valve closing, in the 4S cycle.
- As in the 4-stroke engine, a homogeneous mixture of air, gasoline vapor, and burnt gas is generated within the cylinder before the start of combustion

A further condition for reproducing the in-cylinder pressure diagram measured on the RCCI single-cylinder demonstrator is to keep the same amount of trapped air and burnt gas. To achieve this purpose, it is necessary to design a specific gas-dynamic system for the 2S engine, shown in Figure 7.

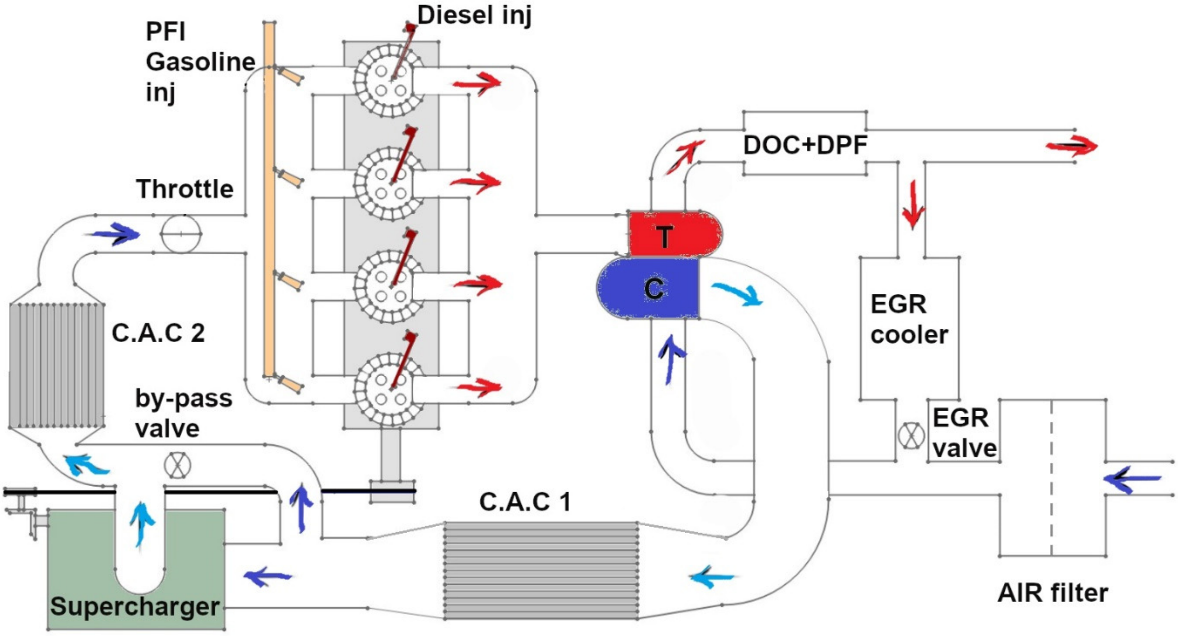


**Figure 7.** Layout of the 2-stroke RCCI engine.

The main aspects considered in the project are summarized in the following.

- Inlet ports and manifold: for each cylinder, a set of 12 piston-controlled ports is fed by a compact manifold, wrapped around the liner, as visible in Figure 8;
- Supercharging system made up of a variable geometry turbocharger (turbine in red, compressor in blue, Figure 7), coupled to a mechanical supercharger, installed after the dynamic compressor and the first Charge air Cooler (C.A.C. 1). A second intercooler (C.A.C. 2) is located between the supercharger and the intake plenum. In this system, the gas flow rate across the cylinders can be regulated by varying both the turbine rack and the area of the bypass valve installed on the supercharger;
- Exhaust manifold, upstream of the turbine: assuming an even firing interval of 90°, the shape of the manifold is designed to prevent the negative effects of interference among cylinders, without damping the kinetic energy of the exhaust flow, feeding the turbine;
- Exhaust gas recirculation: besides the conventional low pressure EGR system (linking the turbine outlet to the compressor inlet, through a cooler), the amount of burnt gas within the cylinder depends on the actuation law of the exhaust valve;
- Gasoline injection system: the low reactivity fuel is supposed to be injected in the intake manifold, at a proper timing, so that a negligible amount of fuel is lost through the exhaust valves, during the scavenging process. The optimization of the gasoline injection system is beyond the scope of this study, and it must be addressed with the support of a further 3D-CFD analysis.

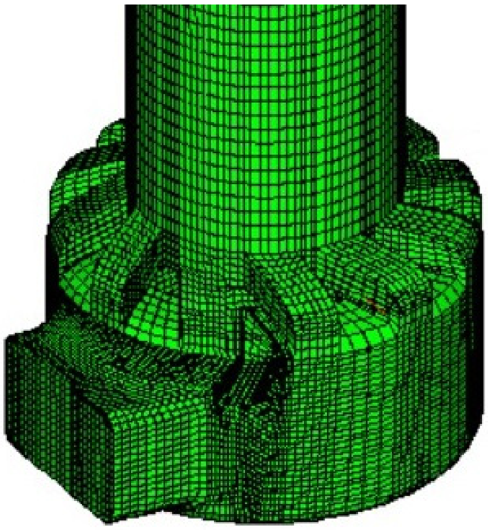

**Figure 8.** Inlet manifold and ports.

Assuming the engine speed and the mass flow rates of gasoline and diesel fuel as independent parameters, the calibration of the gas-dynamic system is far from trivial, due to the high number of control parameters: (1) Turbine rack; (2) throttle angle; (3) opening of the bypass valve on the supercharger; (4) EGR valve opening area; (5) opening of the exhaust flap (a valve installed after the turbine for controlling the amount of low pressure EGR); (6) timing of the exhaust valves.

1D-CFD simulation is the most suitable tool to address the setup of these parameters, as well as to drive the design of the engine components.

The construction of the simulation model is based on the experience of the authors in similar projects [24, 25, 27–31]. The modeling of the scavenging process is based on the 3D-CFD simulation carried out on a 2S engine with the same cylinder design. For Friction Mean Effective Pressure (FMEP), it is assumed that this parameter is halved when passing from a 4S to a 2S cycle. Obviously, the burn rate at each operating condition corresponds to the experimental curve measured on the RCCI prototype.

After the construction of the numerical model at full load (defined by the maximum amount of fuel in RCCI mode), the following parameters have been optimized for the maximization of brake thermal efficiency:

- Height of the inlet ports (timing);
- Opening duration and maximum lift of the exhaust valves;
- Size of the turbocharger;
- Size and transmission ratio of the supercharger;
- Layout and characteristic dimensions of the exhaust manifold, before the turbine;
- Characteristic dimensions of the intake manifold.

Table 4 reviews the main characteristics of the optimized 2S engine.

**Table 4.** Main characteristics of the optimized 2S engine.

| Parameter | Unit | |
|---|---|---|
| Bore × stroke | mm | 83 × 90.4 |
| Compression ratio | # | 16.5 |
| N° of cylinders | # | 4 |
| Total displacement | L | 1.96 |
| N° of exhaust valves | # | 4 |
| Exhaust valve diameter (inner seat) | mm | 20 |
| Exhaust valve opening duration | °CA | 156 |

| | | |
|---|---|---|
| Exhaust valve max. lift | mm | 7.6 |
| Exhaust valve opening | °CA ATDC | 96 |
| Exhaust valve closing | °CA ATDC | 252 |
| N° of inlet ports | # | 12 |
| Width of each inlet port | mm | 14 |
| Height of each inlet port | mm | 9.7 |
| Inlet port opening | °CA ATDC | 135 |
| Inlet port closing | °CA ATDC | 225 |
| Max. reduced mass flow rate of the supercharger | kg/s×K$^{0.5}$/bar | 3.36 |
| Max. reduced mass flow rate of the compressor | kg/s×K$^{0.5}$/bar | 4.04 |
| Max. reduced mass flow rate of the turbine | kg/s×K$^{0.5}$/bar | 1.95 |

It is very important to notice that the 2S engine may be further optimized. As an example, different types of valveless engines could be developed, adopting piston-controlled ports and a brand-new combustion system [24, 25, 27–31]. Even maintaining the uniflow design, the combustion chamber could be redesigned for the new combustion patterns. However, the purpose of the study was not to develop the best possible 2S RCCI design, but to evaluate the advantages for an RCCI engine, when switching from a 4- to a 2-stroke cycle, maintaining all other conditions as close as possible.

## 5. 2S vs. 4S RCCI Engine at Full Load

In this section, a comparison at full load among the standard 4S diesel engine (referred to as 4S_STD, blue), the modified 4S RCCI unit (4S_RCCI, red) and the new 2S RCCI solution (2S_RCCI, green) is presented. For both RCCI engines, the set of full load conditions corresponds to the operating points 3, 6, 9, 12, and 15 of Table 3.

The operating conditions applied to all simulations are:

- Engine speed from 1500 to 3500 rpm, by steps of 500 rpm;
- Experimental burn rates.

The engines also share the following constraints:

- In-cylinder peak pressure: 190 bar;
- Peak of pressure rise rate: 13 bar/deg.

Figure 9 shows the brake performance (torque and power) of the engines. As expected, at low speed the brake output of 4S_RCCI is about halved, in comparison to 4S_STD, mainly because of the constraint on the peak of the pressure rise rate (a further increase of the fuel rate would cause an engine failure). The 2S cycle helps recover a part of the gap, but not all of it. At high speed, 2S_RCCI yields the best performance, also in comparison to 4S_STD.

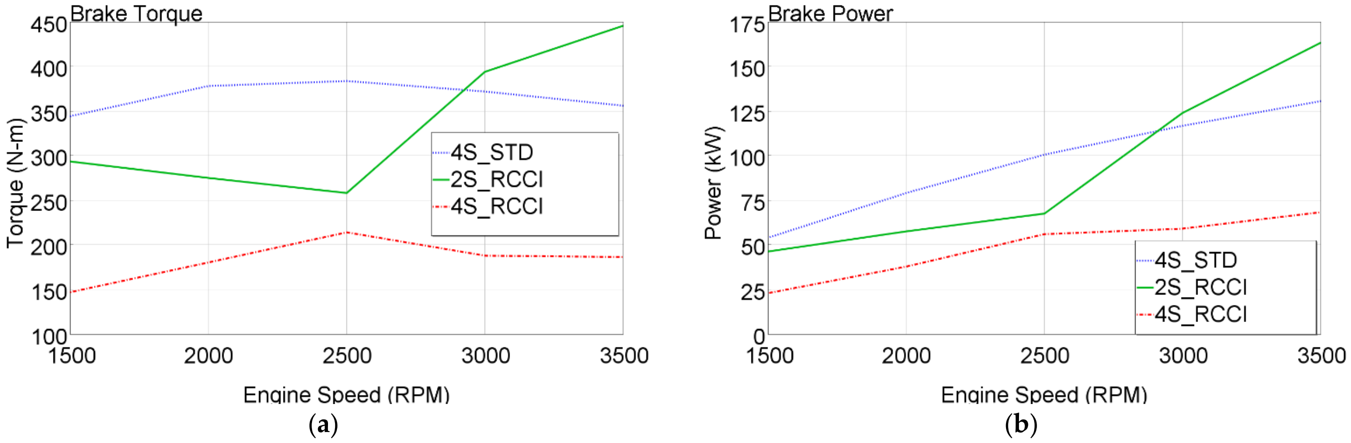


**Figure 9.** Brake torque (**a**) and brake power (**b**) comparison, base diesel engine, 4-stroke RCCI engine and 2-stroke RCCI engine. Operating point 1500–3500 rpm at full load.

The strength of the 2S configuration at high speed is more evident considering the BMEP and GIMEP curves of Figure 10: despite the higher brake torque and power, the cylinder mechanical load, expressed in particular by GIMEP, is much lower than in 4S_STD (16–17 bar vs. 26 bar), and slightly lower than in 4S_RCCI.

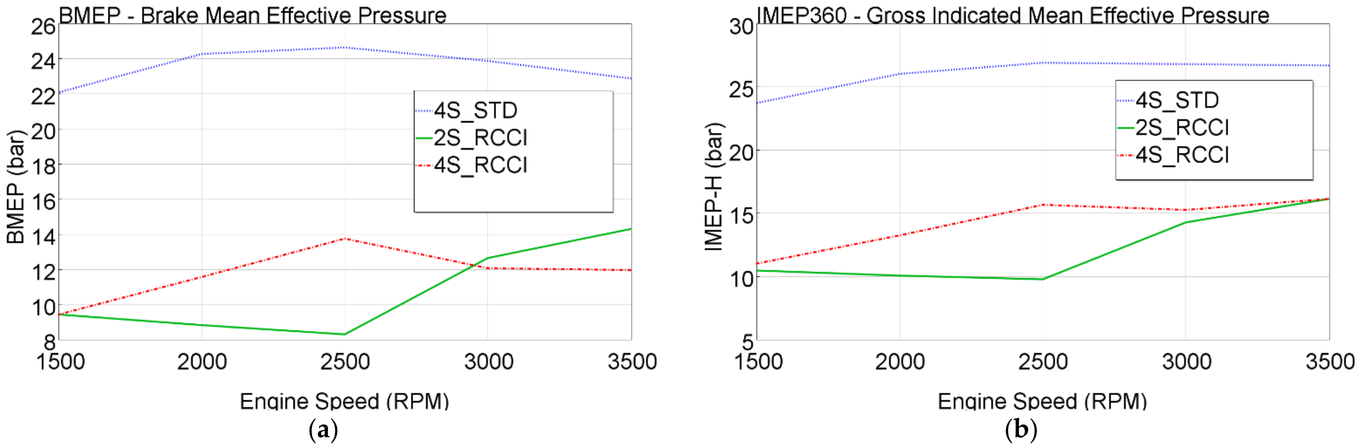


**Figure 10.** BMEP (**a**) and GIMEP (**b**) comparison between base diesel engine, 4-stroke RCCI engine and 2-stroke RCCI engine. Operating point 1500–3500 rpm at full load.

The fuel conversion efficiency of the engines was analyzed by means of the following set of parameters:

- Gross indicated efficiency: ratio of the indicated work done over the compression and expansion strokes (referred to as gross work) to the fuel energy (product of fuel mass and fuel lower heating value);
- Pumping efficiency: ratio of the net indicated work done over the whole cycle to the gross work (for the 2-stroke cycle, the net work is calculated as the difference between the cycle work and the work adsorbed by the supercharger);
- Mechanical efficiency: ratio of the brake work to the net indicated work.

Obviously, the brake thermal efficiency is the product of the three efficiency parameters.

Looking at Figure 10, the highest values of gross indicated efficiency belong to 4S_RCCI. The curve corresponding to 2S_RCCI is shifted down, but it remains always above 4S_STD, except at 1500 rpm. This outcome can be explained considering that RCCI combustion improves the efficiency of the thermodynamic cycle (heat release closer to the isochoric process), in comparison to the standard diesel combustion. However, in the 2S cycle, the expansion stroke is interrupted earlier by the opening of the exhaust valves.

When considering the friction and pumping losses that pass from gross indicated thermal efficiency to brake thermal efficiency, the situation changes a little bit. At high speed, the 2S cycle yields the maximum brake efficiency, thanks to the lowest friction and pumping losses (see also Figure 11); conversely, at medium and low speeds, 2S_RCCI is penalized by the slip of fresh charge through the exhaust during the scavenging process. Even if the amount of lost gasoline is negligible, the work done by the mechanical supercharger to push the excess air and recirculated exhaust gas within the cylinder is a burden for the pumping efficiency of the engine.

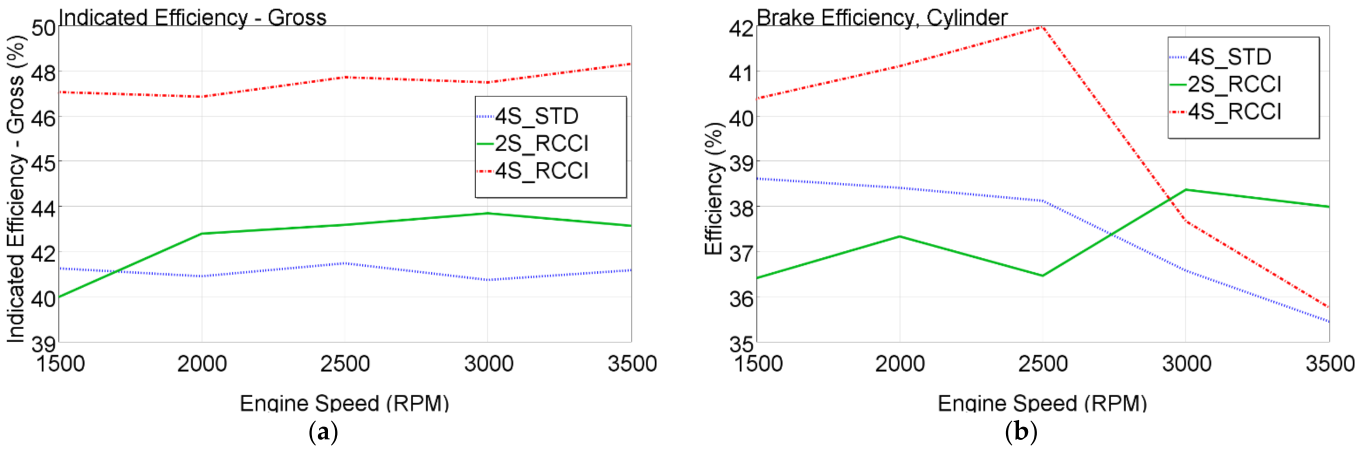


**Figure 11.** Indicated efficiency (**a**) and brake efficiency (**b**) comparison between base diesel engine, 4-stroke RCCI engine and 2-stroke RCCI engine. Operating point 1500–3500 rpm at full load.

The drop in pumping efficiency found on 4S_RCCI over 2500 rpm is due to the high EGR rates required by this combustion mode. While in a standard diesel engine EGR is not necessary at full load, here the target of recirculation rate can be obtained only by throttling the exhaust flow, downstream of the turbine (in order to increase the pressure differential between intake and exhaust). As a result, the engine back-pressure significantly increases, generating higher pumping losses. This issue is not observed in the 2S engine, since the amount of exhaust gas within the cylinder can be controlled simply by varying the exhaust valves timing.

Regarding mechanical efficiency (Figure 12) the relatively low values shown by 4S_RCCI are due to the higher ratio of friction work to indicated work: while the former is almost independent of the brake output, the latter is low when the brake torque is low.

Finally, Figure 13 presents a comparison among the three engines in terms of brake-specific emissions. For the diesel engine, the parameters are directly measured at the dynamometer bench, whereas for the RCCI versions they are calculated. The calculation is based on the experimental measure on the RCCI prototype of the gross indicated specific quantity (i.e., the mass flow rate of pollutant divided by the gross indicated power), and the calculation by GT-Power of pumping and mechanical efficiencies. It is supposed that the gross indicated specific emissions do not change when passing from the 4S to the 2S cycle. The hypothesis is supported by the fact that both engines have the same identical combustion chamber, the same composition of the trapped charge, the same flow field within the cylinder, the same diesel injection strategy, and the same thermodynamic conditions within the cylinder at the combustion onset; therefore, combustion patterns should be identical.

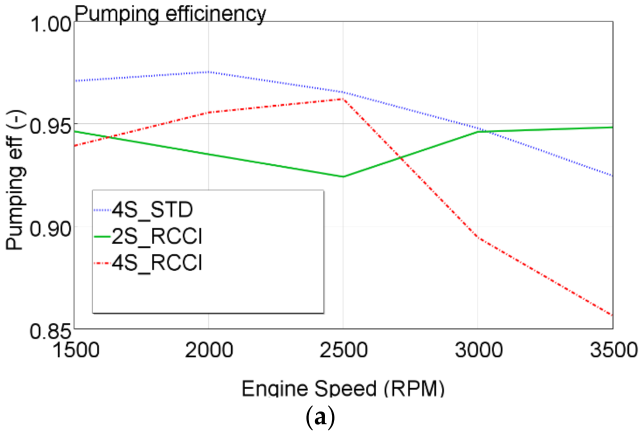


**Figure 12.** Pumping efficiency (**a**) and Mechanical efficiency (**b**) comparison between base diesel engine, 4-stroke RCCI engine, and 2-stroke RCCI engine. Operating point 1500–3500 rpm at full load.

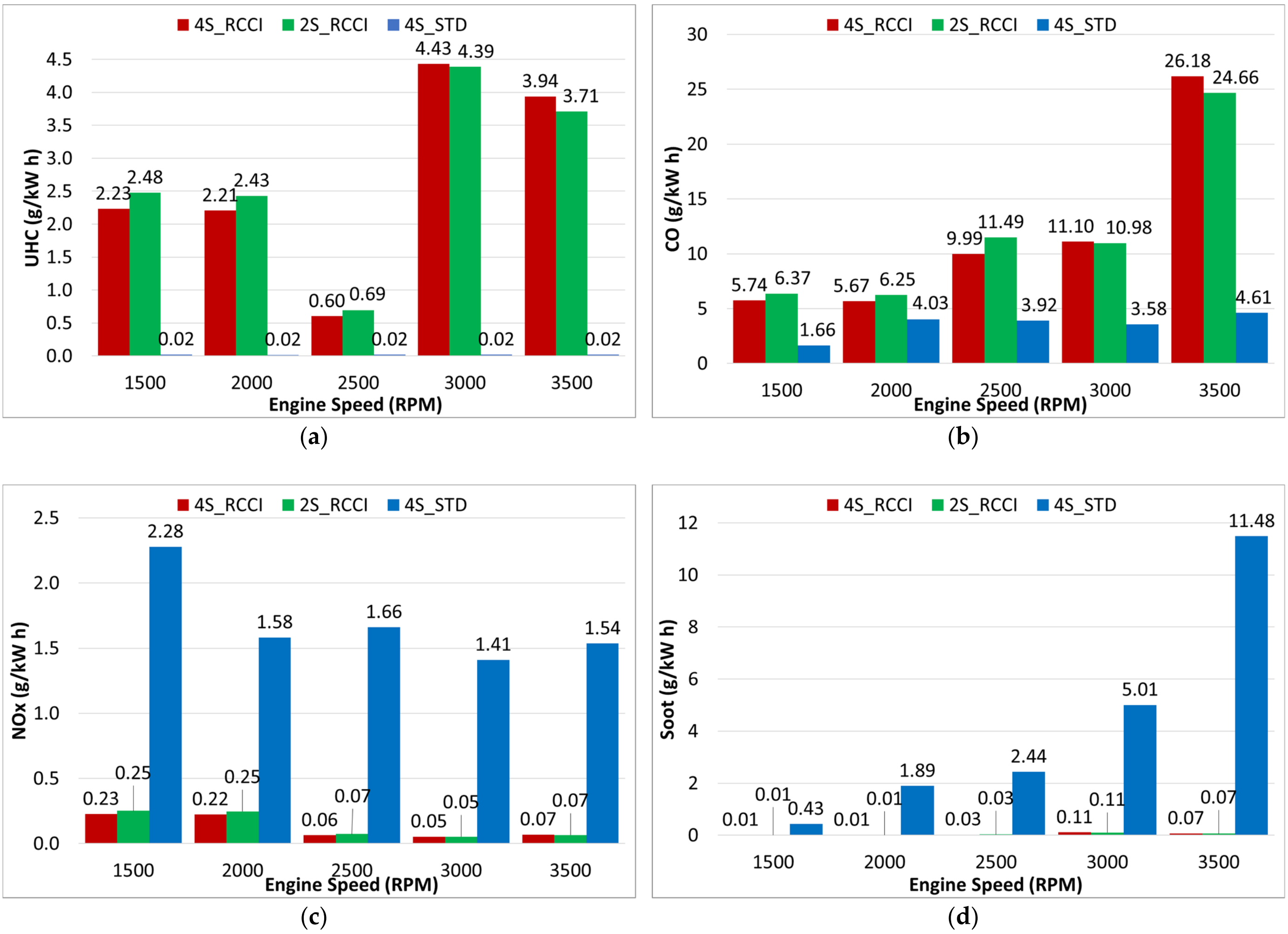

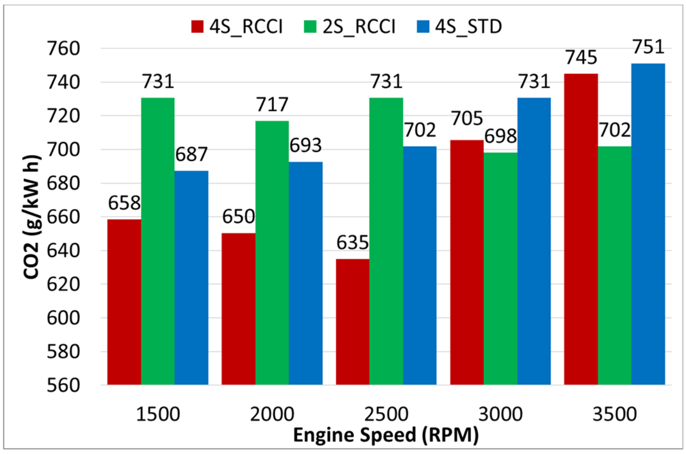


(**e**)

**Figure 13.** Brake-specific emissions comparison: Specific UHC (**a**), Specific CO (**b**), Specific $NO_x$, (c), Specific Soot (**d**), Specific $CO_2$ (**e**)

The brake-specific emissions correspond to the gross indicated specific emission, divided by the product of pumping and mechanical efficiency.

The comparison provides the main results listed below:

- The 2S engine maintains a huge advantage in terms of $NO_x$ and soot emissions observed on the 4S version; RCCI combustion is confirmed to be almost $NO_x$-less and soot-less, as found by many other researchers;
- The drawback of both RCCI engines consists in the strong increase of UHC and CO; this outcome is also typically found in the literature. However, in absolute terms, the concentration of these pollutants is lower or comparable to a conventional SI engine at full load; moreover, they can be easily managed by using a specific oxidation catalyst;
- $CO_2$ emissions are almost perfectly proportional to brake thermal efficiency, due to the similar chemical composition of gasoline and diesel fuel; therefore, at low and medium speed 4S_RCCI has the lowest carbon footprint, while at high speed 2S_RCCI takes the lead.

## 6. Conclusions

The numerical study presented in this paper is based on a comprehensive experimental campaign carried out on a four-cylinder 4-stroke 2.0 L diesel engine. Performance and emissions were measured for two configurations: Standard diesel and "3 + 1", i.e., with one cylinder operating in RCCI mode (gasoline and diesel) and the other three cylinders running on diesel mode. For each operating condition in RCCI mode, a specific calibration was carried out, in order to minimize pollutant emissions (in particular $NO_x$ and soot) and fuel consumption (therefore, also $CO_2$).

The experimental data were used to build and calibrate a 1D-CFD engine model of an RCCI 4-stroke four-cylinder engine. The maximum brake performance of this engine was found to be limited by the constraints on peak cylinder pressure (190 bar) and on peak of pressure rate rise (13 bar/°).

Therefore, a 2-stroke engine, with the same combustion system as the 4-stroke unit, was virtually developed, with the support of 1D-CFD simulation and of empirical assumptions. The maximum care was devoted to reproduce within the 2S engine cylinders with the same identical conditions of the tested RCCI engine (same geometry of the combustion chamber, same composition of the charge, same in-cylinder flow field, same diesel injection strategy).

Under these hypotheses, it can be assumed that gross indicated specific emissions are identical between 2- and 4-stroke. Therefore, brake-specific emissions of the RCCI engines can be calculated by adjusting the experimental data with the support of 1D-CFD simulation, which provides the values of mechanical and pumping efficiency.

The numerical comparison at full load among the standard diesel, the 4-stroke RCCI, and the 2-stroke RCCI yielded the following main results:

- $NO_x$ and soot brake-specific emissions are reduced by at least one order of magnitude when passing from diesel to RCCI, both in 4-stroke and 2-stroke;
- Conversely, UHC and CO increase, but they can be easily managed by a cost-effective oxidation catalyst;
- Brake thermal efficiency (and then the carbon footprint) is always improved when switching from diesel to RCCI, in the 4-stroke cycle;
- In comparison to the 4-stroke RCCI engine, the 2-stroke engine provides an almost double brake torque and power;
- At high speed, the 2-stroke RCCI engine has the highest power output and the highest brake thermal efficiency.

In conclusion, the 2-stroke cycle can be an ideal platform for developing RCCI combustion systems, considering that the reduction of pollutant emissions and fuel consumption, experimentally and theoretically observed by most researchers, can be obtained without significant penalization on brake performance.

**Author Contributions:** Conceptualization, E.M., C.A.R., L.M., S.C., F.L. and F.S.; methodology, E.M., C.A.R., L.M., S.C., F.L. and F.S.; software, E.M., C.A.R., L.M., S.C., F.L. and F.S.; validation, E.M., C.A.R., L.M., S.C., F.L. and F.S.; formal analysis, E.M., C.A.R., L.M., S.C., F.L. and F.S.; investigation, E.M., C.A.R., L.M., S.C., F.L. and F.S.; resources, E.M., C.A.R., L.M., S.C., F.L. and F.S.; data curation, E.M., C.A.R., L.M., S.C., F.L. and F.S.; writing—original draft preparation, E.M., C.A.R., L.M., S.C., F.L. and F.S.; writing—review and editing, E.M., C.A.R., L.M., S.C., F.L. and F.S.; visualization, E.M., C.A.R., L.M., S.C., F.L. and F.S.; supervision, E.M., C.A.R. and L.M. All authors have read and agreed to the published version of the manuscript.

**Funding:** This research received no external funding.

**Acknowledgments:** GAMMA-TECHNOLOGIES is acknowledged for the GT-SUITE license granted to the University of Modena and Reggio Emilia.

**Conflicts of Interest:** The authors declare no conflict of interest.

## Definitions/Abbreviations

| | |
|---|---|
| # | Number |
| 2S | 2-Stroke |
| 2S_RCCI | 2-Stroke RCCI engine |
| 4S | 4-Stroke |
| 4S_RCCI | 4-Stroke RCCI engine |
| 4S_STD | 4-Stroke Standard Diesel engine |
| ATDC | After Top Dead Center |
| BEV | Battery Electric Vehicles |
| BMEP | Brake Mean Effective Pressure |
| BTE | Brake Thermal Efficiency |
| CA | Crank Angle |
| CAC | Charge Air Cooler |
| CDC | Conventional Diesel Combustion |
| CFD | Computational Fluid Dynamics |
| CI | Compression Ignition |
| CO | Carbon Monoxide |
| $CO_2$ | Carbon Dioxide |
| CR | Compression Ratio |
| DMDF | Dual-Mode Dual-Fuel |
| DOC | Diesel Oxidation Catalyst |
| DPF | Diesel Particulate Filter |

| | |
|---|---|
| ECU | Electronic Control Unit |
| EGR | Exhaust Gas Recirculation |
| FMEP | Friction Mean Effective Pressure |
| GA | Genetic Algorithm |
| GHG | Greenhouse Gas |
| GIMEP | Gross Indicated Mean Effective Pressure |
| HEV | Hybrid Electric Vehicles |
| HP EGR | High Pressure EGR line |
| ICE | Internal Combustion Engine |
| IMEP | Indicated Mean Effective Pressure |
| LP EGR | Low Pressure EGR line |
| LTC | Low Temperature Combustion |
| $NO_x$ | Nitrogen Oxides |
| PM | Particulate Matter |
| PPRR | Peak Pressure Rise Rate |
| RCCI | Reactivity Controlled Compression Ignition |
| SCR | Selective Catalytic Reduction |
| SI | Spark Ignition |
| SOI | Start Of Injection |
| UHC | Unburnt Hydrocarbons |
| VGT | Variable Geometry Turbine |
| VSA | Variable Swirl Actuator |
| VVA | Variable Valve Actuation |

## References


1. Ritchie, H.; Roser, M. $CO_2$ and Greenhouse Gas Emissions. Our World in Data. May 2020. Available online: https://ourworldindata.org/co2-and-other-greenhouse-gas-emissions (accessed on 12 September 2021).
2. Global Warming of 1.5 °C. Available online: https://www.ipcc.ch/sr15/ (accessed on 12 September 2021).
3. Mitigation. UN Climate Change Conference (COP26) at the SEC—Glasgow 2021. Available online: https://ukcop26.org/cop26-goals/mitigation/ (accessed on 2 December 2021).
4. COP26 Goals. UN Climate Change Conference (COP26) at the SEC—Glasgow 2021. Available online: https://ukcop26.org/cop26-goals/ (accessed on 2 December 2021).
5. Reitz, R.D.; Ogawa, H.; Payri, R.; Fansler, T.; Kokjohn, S.; Moriyoshi, Y.; Agarwal, A.; Arcoumanis, D.; Assanis, D.; Bae, C.; et al. IJER editorial: The future of the internal combustion engine. *Int. J. Engine Res.* **2020**, *21*, 3–10. https://doi.org/10.1177/1468087419877990.
6. Agarwal, A.K.; Singh, A.P.; Maurya, R.K. Evolution, challenges and path forward for low temperature combustion engines. *Prog. Energy Combust. Sci.* **2017**, *61*, 1–56. https://doi.org/10.1016/j.pecs.2017.02.001.
7. Hanson, R.M.; Kokjohn, S.L.; Splitter, D.; Reitz, R.D. An Experimental Investigation of Fuel Reactivity Controlled PCCI Combustion in a Heavy-Duty Engine. *SAE Int. J. Engines* **2010**, *3*, 700–716. https://doi.org/10.4271/2010-01-0864.
8. Curran, S.; Prikhodko, V.; Cho, K.; Sluder, C.S.; Parks, J.; Wagner, R.; Kokjohn, S.; Reitz, R.D. In-Cylinder Fuel Blending of Gasoline/Diesel for Improved Efficiency and Lowest Possible Emissions on a Multi-Cylinder Light-Duty Diesel Engine. In Proceedings of the SAE 2010 Powertrains Fuels & Lubricants Meeting, San Diego, CA, USA, 25–27 October 2010; https://doi.org/10.4271/2010-01-2206.
9. Kokjohn, S.L.; Hanson, R.; Splitter, D.; Kaddatz, J.; Reitz, R.D. Fuel Reactivity Controlled Compression Ignition (RCCI) Combustion in Light- and Heavy-Duty Engines. *SAE Int. J. Engines* **2011**, *4*, 360–374. https://doi.org/10.4271/2011-01-0357.
10. Kokjohn, S.L.; Hanson, R.M.; Splitter, D.; Reitz, R.D. Fuel reactivity controlled compression ignition (RCCI): A pathway to controlled high-efficiency clean combustion. *Int. J. Engine Res.* **2011**, *12*, 209–226. https://doi.org/10.1177/1468087411401548.
11. Benajes, J.; Molina, S.; García, A.; Belarte, E.; Vanvolsem, M. An investigation on RCCI combustion in a heavy duty diesel engine using in-cylinder blending of diesel and gasoline fuels. *Appl. Therm. Eng.* **2014**, *63*, 66–76. https://doi.org/10.1016/j.applthermaleng.2013.10.052.
12. Reitz, R.D.; Duraisamy, G. Review of high efficiency and clean reactivity controlled compression ignition (RCCI) combustion in internal combustion engines. *Prog. Energy Combust. Sci.* **2015**, *46*, 12–71. https://doi.org/10.1016/j.pecs.2014.05.003.
13. Kokjohn, S.L.; Reitz, R.D.; Splitter, D.; Musculus, M.P.B. Investigation of Fuel Reactivity Stratification for Controlling PCI Heat-Release Rates Using High-Speed Chemiluminescence Imaging and Fuel Tracer Fluorescence. *SAE Int. J. Engines* **2012**, *5*, 248–269. https://doi.org/10.4271/2012-01-0375.
14. Tang, Q.; Liu, H.; Li, M.; Geng, C.; Yao, M. Multiple optical diagnostics on effect of fuel stratification degree on reactivity controlled compression ignition. *Fuel* **2017**, *202*, 688–698. https://doi.org/10.1016/j.fuel.2017.04.136.

15. Delvescovo, D.; Kokjohn, S.; Reitz, R. The Effects of Charge Preparation, Fuel Stratification, and Premixed Fuel Chemistry on Reactivity Controlled Compression Ignition (RCCI) Combustion. *SAE Int. J. Engines* **2017**, *10*, 1491–1505. https://doi.org/10.4271/2017-01-0773.
16. Liu, H.; Tang, Q.; Yang, Z.; Ran, X.; Geng, C.; Chen, B.; Feng, L.; Yao, M. A comparative study on partially premixed combustion (PPC) and reactivity controlled compression ignition (RCCI) in an optical engine. *Proc. Combust. Inst.* **2018**, *37*, 4759–4766. https://doi.org/10.1016/j.proci.2018.06.004.
17. Paykani, A.; Kakaee, A.-H.; Rahnama, P.; Reitz, R.D. Progress and recent trends in reactivity-controlled compression ignition engines. *Int. J. Engine Res.* **2015**, *17*, 481–524. https://doi.org/10.1177/1468087415593013.
18. Ma, S.; Zheng, Z.; Liu, H.; Zhang, Q.; Yao, M. Experimental investigation of the effects of diesel injection strategy on gasoline/diesel dual-fuel combustion. *Appl. Energy* **2013**, *109*, 202–212. https://doi.org/10.1016/j.apenergy.2013.04.012.
19. Molina, S.; García, A.; Pastor, J.-M.; Belarte, E.; Balloul, I. Operating range extension of RCCI combustion concept from low to full load in a heavy-duty engine. *Appl. Energy* **2015**, *143*, 211–227. https://doi.org/10.1016/j.apenergy.2015.01.035.
20. Kavuri, C.; Kokjohn, S.L. Computational optimization of a reactivity controlled compression ignition (RCCI) combustion system considering performance at multiple modes simultaneously. *Fuel* **2017**, *207*, 702–718. https://doi.org/10.1016/j.fuel.2017.06.071.
21. Benajes, J.; García, A.; Monsalve-Serrano, J.; Boronat, V. Achieving clean and efficient engine operation up to full load by combining optimized RCCI and dual-fuel diesel-gasoline combustion strategies. *Energy Convers. Manag.* **2017**, *136*, 142–151. https://doi.org/10.1016/j.enconman.2017.01.010.
22. Xu, G.; Monsalve-Serrano, J.; Jia, M.; García, A. Computational optimization of the dual-mode dual-fuel concept through genetic algorithm at different engine loads. *Energy Convers. Manag.* **2020**, *208*, 112577. https://doi.org/10.1016/j.enconman.2020.112577.
23. GT-SUITE. Gamma Technologies.Available online: https://www.gtisoft.com/gt-suite/ (accessed on 24 January 2022).
24. Ferrari, G. *Internal Combustion Engines*; Società Editrice Esculapio: Bologna, Italy, 2014.
25. Mattarelli, E.Virtual design of a novel 2-Stroke HSDI diesel engine. *Int. J. Engine Res.* **2009**, *10*, 1468–0874.
26. Rinaldini, C.A.; Mattarelli, E.; Golovitchev, V. CFD Analyses on 2-Stroke High Speed Diesel Engines. *SAE Int. J. Engines* **2011**, *4*, 2240–2256. https://doi.org/10.4271/2011-24-0016.
27. Mattarelli, E.; Cantore, G.; Rinaldini, C.A.Advances in the design of two-stroke, high speed, compression ignition engines. *Adv. Intern. Combust. Engines Fuel Technol.* **2013**, 149–182. https://doi.org/10.5772/54204.
28. Mattarelli, E.; Rinaldini, C.A.; Savioli, T. Port Design Criteria for 2-Stroke Loop Scavenged Engines. *SAE Tech. Pap.* **2016**, *1*. https://doi.org/10.4271/2016-01-0610.
29. Mattarelli, E.; Rinaldini, C.A.; Patroncini, P. Commercial Vehicles: New Diesel Engine Concepts for Euro VI and Beyond. *SAE Tech. Pap.* **2017**. https://doi.org/10.4271/2017-26-0034.
30. Mattarelli, E.; Rinaldini, C.; Savioli, T.; Cantore, G.; Warey, A.; Potter, M.; Gopalakrishnan, V.; Balestrino, S. Scavenge Ports Ooptimization of a 2-Stroke Opposed Piston Diesel Engine. *SAE Tech. Pap.* **2017**, *1*. https://doi.org/10.4271/2017-24-0167.
31. Mattarelli, E.; Cantore, G.; Rinaldini, C.A.; Savioli, T. Combustion System Development of an Opposed Piston 2-Stroke Diesel Engine. *Energy Procedia* **2017**, *126*, 1003–1010. https://doi.org/10.1016/j.egypro.2017.08.268.